

CORRELATION ANALYSIS OF ELECTROSTATIC FLUCTUATION BETWEEN CENTRAL AND END CELLS IN GAMMA 10

Yoshiaki Miyata, Masayuki Yoshikawa, Youhei Oono, Fumiaki Yaguchi, Makoto Ichimura, Tatsuya Murakami and Tsuyoshi Imai

*Plasma Research Center, University of Tsukuba, Tsukuba, Ibaraki, 305-8577 Japan
miyata@prc.tsukuba.ac.jp*

The electrostatic fluctuation was observed by a heavy ion beam probe (HIBP) at the central cell in the GAMMA 10 tandem mirror. The fluctuation of the end plates settled at both side of GAMMA 10 was observed. In the plasma, as increasing of the electrostatic fluctuation, decrease of the diamagnetism and electron density was observed. The radial profile of particle transport induced by fluctuations increased substantially. A strong correlation between the potential fluctuations measured by HIBP and end plates was observed. The electrostatic fluctuation propagated from the central cell to end cell.

I. INTRODUCTION

Fluctuations are observed in some magnetic confinement devices. The fluctuations due to the instabilities cause the anomalous transports¹. The drift waves called the universal instability due to the plasma density gradient have been observed in many devices²⁻⁴. It is quite important to study the plasma particle transport across the confinement magnetic field as a result of the fluctuation due to instabilities in plasmas. In the GAMMA 10 tandem mirror, the electrostatic and magneto hydrodynamic fluctuations are observed by some measurement systems and they are related to the radial transport⁵. The decreasing of the plasma stored energy due to the radial transport was also observed.

Experiments were conducted in the GAMMA 10 tandem mirror. The plasma is created by plasma guns at the both sides of GAMMA 10, and heated and sustained using ion cyclotron range of frequency (ICRF) heating systems. In the standard operation the length and the magnetic field strength at the mid-plane of the central cell are 6.0 m and 0.41 T, respectively. The anchor cells are located at both sides of the central cell and consist of minimum-B mirror field which is produced by base ball coil. The plug/barrier cells are located outside of anchor cells, where the electron confinement potentials and ion confinement potentials are produced using electron cyclotron resonance heating (ECRH). The end plates made of stainless steel are settled at both end sides of

GAMMA 10. The plasma touches the end plates along the magnetic field. The core plasma potential is observed by the heavy ion beam probe (HIBP) at central cell in GAMMA 10. The electrostatic fluctuations are observed by HIBP during ICRF heating^{6,7}.

In this paper, we show the effect of radial particle transport induced by the fluctuations measured by a HIBP. We show the result of the potential fluctuation of the end plates measurement. The correlation between the potential fluctuation measured by HIBP and that of end plates was assessed.

II. GOLD NEUTRAL BEAM PROBE

A beam probe is a useful tool on the basis of the energy conservation of a heavy ion beam for the potential and fluctuation measurements. The beam probe system consists of two parts. One is a beam source which produces a high energy ion beam. The other is a beam detector using an electrostatic energy analyzer. The incident beam and the ionized ion beam in plasma are called the primary and secondary beams, respectively. The basic principle of the potential measurement is a conservation law between the beam energy and the plasma potential. When the energy of the secondary beam is measured, the plasma potential is estimated from the change of the beam energy as follows:

$$\phi = \frac{1}{Ze} (E_{secondary} - E_{primary})$$

Where $E_{primary}$ and $E_{secondary}$ are the energy of the primary and secondary beams, respectively. Also, Z is the change of the ion charge number at ionization point, and ϕ is the plasma potential at the arbitrary ionization point. The ionization point of the detected secondary beam is limited to the small volume due to the beam slit in front of the analyzer. The secondary beam has the information on not only the plasma potential but also the electron density. The secondary beam current depends on the electron density at the ionization point. Therefore, it is possible to

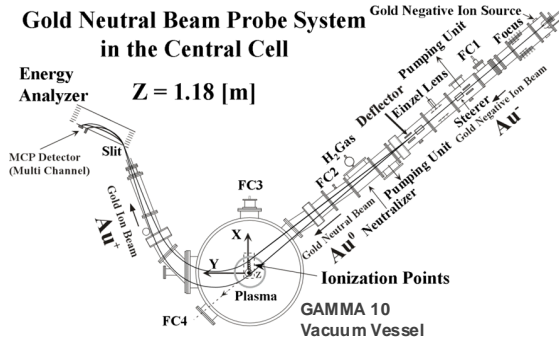


Fig.1 Gold neutral beam probe system in the central cell of the GAMMA 10 tandem mirror. (Here, the z -axis is in the perpendicular direction to the plane).

measure the density and potential by using the beam probes.

A 12 keV gold neutral beam probe (GNBP) with same capabilities as HIBP operates on the GAMMA 10 tandem mirror. Figure 1 shows the schematic of the GNBP system. The negative Au^- beam is produced by the Cs sputtering ion source. After acceleration and focusing, negative beam is neutralized on a gas (H_2) target. The resulted primary Au^0 beam is injected into the plasma. The energy and incident angle of the primary beam passing the plasma center are about 12 keV and 40 degree to the horizontal direction, respectively. The incident angle can be changed in vertical and horizontal directions by two electrostatic deflectors arranged before neutralizer. Typical primary beam diameter and current intensity are 5 mm and 2 μA measured by Faraday cup detector, respectively. The secondary beam of Au^+ ions produced in collisions with plasma electrons is analyzed by parallel plate type electrostatic energy analyzer with the incident angle of 45 degree to the ground plate. Secondary ions are detected by microchannel plate with 32 anodes of 2.4 mm width. The plasma density and potential as well as their fluctuations can be measured. It is possible to measure the density and potential fluctuations and phase difference between them at the arbitrary point simultaneously by GNBP.

Small fluctuations give rise to the local transport. If the average value of the local transport is not zero, the net transport is defined as the radial particle flux. In the case of GAMMA 10, the radial particle flux due to the electrostatic fluctuations is defined as $\gamma_{n\phi} \tilde{I} / I \tilde{\phi} \sin \alpha_{n\phi}$.

Here, $\gamma_{n\phi}$, \tilde{I} , $\tilde{\phi}$ and $\alpha_{n\phi}$ are the coherence, the density fluctuation, potential fluctuation and the phase difference between the density and the potential fluctuations, respectively⁵.

III. END PLATE MEASUREMENT

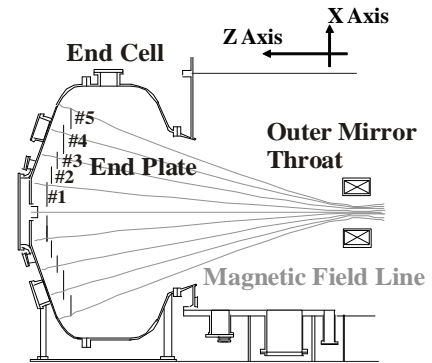


Fig.2 Schematic view of end plates settled at both side of GAMMA 10. The end plates consist of some divided plates. (Here, the Y -Axis is in the perpendicular direction to the plane).

The end plates (EP) made of stainless steel is settled at both end sides of GAMMA 10 for receiving the end loss plasma. The EPs consist of some divided plates made of stainless steel. The EPs are divided into five sections in radial direction and connected to ground through the 1 M Ω of cement resistor. The EP #1, #2, #3 and #4 cover the region of radius compared at central cell ~ 5.5 , $5.5 \sim 7.8$, $7.8 \sim 11$ and $11 \sim 16$ cm, respectively. The #1, #2 and #3 EPs are divided into four. The #4 EPs are divided into eight sections in circumferential direction and normally connected. Figure 2 shows schematic view of EPs system on the west side. The EP potential is affected by changing of the cement resistor. The plasma potential is so high as to reduce the resistance value. Then it is possible to control the radial potential profile in GAMMA 10. We measured the floating potential of each EP by using the 50 Ω of pick-up resistor.

The high-performance analog-digital convertor (ADC) was installed to the EPs and GNBP. The ADC has the resolution of 16 bits and it is possible to measure 16 channels simultaneously. Its sampling frequency is 333 kHz. It is possible to measure the radial fluctuation profile and assess the correlation by loading the EPs of radial position. The fluctuations of EP and GNBP were analyzed by using the sample of 512 points and hanning window.

IV. EXPERIMENTAL RESULTS

After starting up the plasma with the both sides of plasma gun, ICRF heating systems are used in the central cell. The plasma was heated from 50 ms by ICRF heating and increased the ion temperature. In order to study the feature of electrostatic fluctuation, it is necessary to produce the plasma in which the electrostatic fluctuation occurs with adjusting the heating and gas puffing sequences. The electrostatic fluctuation which increases with time was observed by GNBP. We focused attention

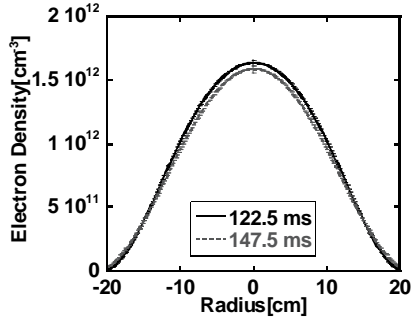


Fig.3 Radial electron density profile measured by microwave interferometer in the central cell.

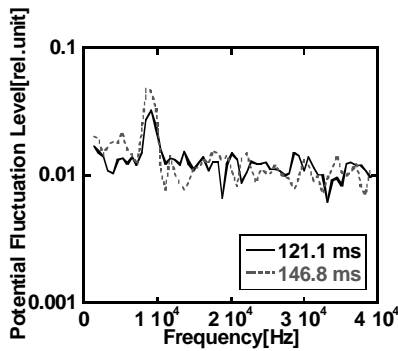


Fig.4 Spectrum of potential fluctuation level near the center by using GNPB at 121.1 and 146.8 ms.

on ICRF heating time at 120 - 130 and 145 - 155 ms because we assess the effects of the radial particle transport. The plasma stored energy decreased with time in spite of ICRF heating at a constant power. The diamagnetism measured by diamagnetic loop depends on the temperature and density. The diamagnetism decreased at rate of 3 % from 120 - 130 to 145 - 155 ms. Figure 3a shows the radial profile of electron density measured by microwave interferometer in the central cell. The electron density decreased inside and increased outside with time. The radial profile of electron density was smoothed.

The potential fluctuation was measured by GNPB at central cell. It is necessary that some plasma shots in which the heating sequence was fixed for discussing the characteristic of fluctuation on radial position. For measuring the radial profile we change the measurement point every shot by deflecting voltage in the ion source of GNPB. Figure 4 shows the spectrum of potential fluctuation level near the center by using GNPB at 121.1 and 146.8 ms. The power spectra was averaged by using root mean square (RMS) averaging. The analysis time interval is almost 1.5 ms. The RMS averaging points are 3. The potential fluctuation level had the peak near 9 kHz and increased from 0.03 - 121.1 ms to 0.05 at 146.8 ms. The fluctuation near 9 kHz was identified by electrostatic probe established in circumferential direction. The

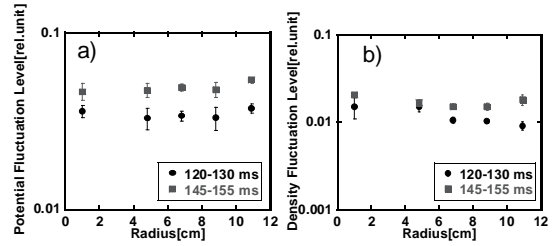


Fig.5 a) Radial profile of potential fluctuation level. b) Radial profile of density fluctuation measured by GNPB.

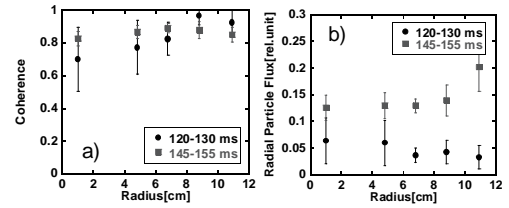


Fig.6 a) Radial profile of coherence between the potential and density fluctuations. b) Radial profile of particle flux calculated using GNPB data.

observed fluctuation was estimated as the drift-type fluctuation with the azimuthally mode number of 2. Previous research has suggested that the drift-type fluctuation occurs strongly in a high plasma pressure case at central cell⁸. Figure 5a and 5b show the radial profile of drift-type potential and density fluctuation level by using GNPB at 120 - 130 and 145 - 155 ms. The fluctuations level is 10 ms averaged. The potential and density fluctuations had the same level in radial direction and increased with time. These results show the drift-type fluctuation has global structure in radial direction. Figure 6a shows the radial profile of coherence between the potential and density fluctuations. The radial profile of coherence was almost 0.8 in radial direction. The radial particle flux due to the phase difference between the potential and density fluctuations was calculated. Figure 6b shows the radial profile of radial particle flux related value calculated by GNPB. This particle flux indicates the local transport at the arbitrary ionization point. The radial particle flux related value was two or three times more from 120 - 130 to 145 - 155 ms. This result indicated that the particle transport increased in radial direction. The decreasing of diamagnetism and varying of electron density was related to the radial particle flux due to the drift-type fluctuation.

The fluctuation of EPs potential was analyzed on the same plasma. Figure 7 shows the spectra of #1 EP potential fluctuation at 121.1 and 146.8 ms. The EP potential fluctuation also had the peak near 9 kHz same as the potential fluctuation measured by GNPB. The EP potential fluctuation level increased from 0.04 at 121.1 ms to 0.08 at 146.8 ms. Figure 8a shows the radial profile of

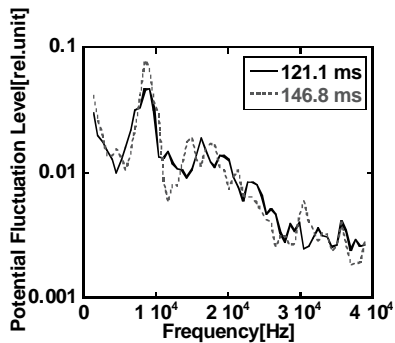


Fig.7 Spectrum of #1 EP potential fluctuation at 121.1 and 146.8 ms.

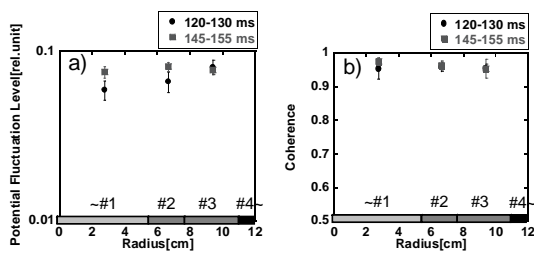


Fig.8 a) Radial profile of potential fluctuation level measured by EP #1 - #3 at 120 - 130 and 145 - 155 ms. b) Radial profile of coherence between potential fluctuations measured by GNB and EPs at 120 - 130 and 145 - 155 ms.

potential fluctuation level by using EP #1, #2 and #3 at 120 - 130 and 145 - 155 ms. The EP potential fluctuations level was 10 ms averaged. These results show that potential fluctuation of EPs also had the same level in radial direction and increased with time.

The drift-type fluctuation may not occur in a low plasma pressure case such as end cell plasma. The correlation between central and end cells was assessed for identifying the fluctuation measured by EPs. Figure 8b shows the radial profile of coherence between the potential fluctuations measured by GNB and EP. We assessed the correlation between the potential fluctuations measured by GNB and EP in same magnetic field line because the fluctuation propagates in magnetic field line. The coherence between central and end cells was almost 0.95 at both 120 - 130 and 145 - 155 ms. The drift-type fluctuation measured at central cell correlated strongly with the fluctuation measured at end cell. This fluctuation at end cell appears identical to the drift-type fluctuation at central cell. These results show that the drift-type fluctuation which produces the radial particle transport propagates from the central cell to the end cell.

V. SUMMARY

The density and potential fluctuations were observed at central cell by using GNB. The potential fluctuation of the end plates settled at both side of GAMMA 10 was

observed. For studying the feature of electrostatic fluctuation, we adjusted the heating and gas puffing sequences. The drift-type fluctuation with azimuthally mode number of 2 near 9 kHz increased, and the plasma stored energy decreased with time. The diamagnetism decreased at rate of 3 % and the radial profile of the particle flux induced by fluctuations was two or three times more from 120 - 130 to 145 - 155 ms. The EP potential fluctuation also had the peak near 9 kHz and increased with time. The correlation between central and end cells was assessed for identifying the fluctuation measured by EPs. The drift-type fluctuation measured at central cell correlated strongly with the fluctuation measured at end cell. The drift-type fluctuation propagated from the central cell to the end cell.

ACKNOWLEDGMENTS

The authors would like to thank members of GAMMA 10 group of the University of Tsukuba for their collaboration. This work was partly supported by the Grant-in-Aid for Young Scientists (B), No. 22740359. This work is performed with the support and under the auspices of the NIFS Collaboration Research Program, NIFS04KUGM009.

REFERENCES

1. B. FISCHER et al., "Experimental study of drift wave turbulence and anomalous transport", Plasma Phys. Control. Fusion 31, 453 (1989).
2. H. W. HENDEL et al., "Collisional Effects in Plasmas-Drift-Wave Experiments and Interpretation", Phys. Rev. Lett. 18, 439 (1967).
3. H. W. HENDEL et al., "Collisional Drift Waves - Identification, Stabilization, and Enhanced Plasma Transport", Phys. Fluids. 11, 2426 (1968).
4. W. HORTON, "Drift waves and transport", Rev. Mod. Phys. 71, 735 (1999).
5. A. KOJIMA et al., "OBSERVATION OF RADIAL TRANSPORT INDUCED BY THE FLUCTUATION MEASURED WITH A GOLD NEUTRAL BEAM PROBE", Trans. Fusion Sci. Tech. 51, 2T, 274 (2007).
6. Y. MIYATA et al., "Study of Radial Particle Flux due to Phase Difference Between Potential and Density Fluctuations", Trans. Fusion Sci. Tech. 55, 168 (2009).
7. Y. MIYATA et al., "Observation of the Effects of Radially Sheared Electric Field by Use of a Gold Neutral Beam Probe", J. Plasma Fusion Res. 2, S1101 (2007).
8. S. TANAKA et al., "Low Frequency fluctuations measured by probes in the GAMMA 10 tandem mirror", Rev. Sci. Instrum. 70, 979 (1999).